

# ANALOG INTEGRATED CIRCUIT DESIGN



DAVID A. JOHNS  
KEN MARTIN

ENGR

TR

7874

J65x

1997



CORNELL UNIVERSITY LIBRARY



3 1924 080 732 385



JAN 13 1998

DATE DUE	
<del>OCT 11 2004</del>	<del>AUG 10 2009</del>
<del>NOV 3 2004</del>	<del>AUG 26 2006</del>
<del>JAN 29 2005</del>	<del>FEB 20 2007</del>
<del>APR 24 2005</del>	<del>DEC 16 2007</del>
<del>MAR 15 2005</del>	<del>FEB 26 2008</del>
<del>SEP 21 2005</del>	<del>MAR 21 2009</del>
<del>DEC 6 2005</del>	<del>JUL 6 2010</del>
<del>FEB 2 2006</del>	<del>FEB 25 2011</del>
<del>JUL 13 2006</del>	<del>MAR 19 2012</del>
	<del>JUN 1 2012</del>

GAYLORD

PRINTED IN U.S.A.

# ANALOG INTEGRATED CIRCUIT DESIGN

---

David Johns

Ken Martin

*University of Toronto*



John Wiley & Sons, Inc.

New York • Chichester • Brisbane  
Toronto • Singapore • Weinheim



*Acquisitions Editor*  
*Marketing Manager*  
*Production Manager*  
*Senior Production Editor*  
*Designer*  
*Manufacturing Manager*  
*Illustration Editor*

Charity Robey  
Jay Kirsch  
Lucille Buonocore  
Tracey Kuehn  
Kevin Murphy  
Mark Cirillo  
Sigmund Malinowski



This book was set in Times Roman by Publication Services and printed and bound by R.R. Donnelley/Crawfordsville. The cover was printed by Lehigh Press.

Recognizing the importance of preserving what has been written, it is a policy of John Wiley & Sons, Inc., to have books of enduring value published in the United States printed on acid-free paper, and we exert our best efforts to that end.

The paper in this book was manufactured by a mill whose forest management programs include sustained yield harvesting of its timberlands. Sustained yield harvesting principles ensure that the number of trees cut each year does not exceed the amount of new growth.

Copyright © 1997, by John Wiley & Sons, Inc.

All rights reserved. Published simultaneously in Canada.

Reproduction or translation of any part of this work beyond that permitted by Sections 107 and 108 of the 1976 United States Copyright Act without the permission of the copyright owner is unlawful. Requests for permission or further information should be addressed to the Permissions Department, John Wiley & Sons, Inc.

***Library of Congress Cataloging-in-Publication Data:***

Johns, David, 1958—  
Analog integrated circuit design / David Johns, Ken Martin.  
p. cm.  
Includes bibliographical references.  
ISBN 0-471-14448-7 (cloth : alk. paper)  
1. Linear integrated circuits—Design and construction.  
I. Martin, Kenneth W. (Kenneth W.) 1952— . II. Title.  
TK7874.J65 1996  
621.3815—dc20

96-34365  
CIP

ISBN 0-471-14448-7

Printed in the United States of America

10 9 8 7 6 5 4 3 2

# Contents

---

<b>CHAPTER 1</b>	<b>INTEGRATED-CIRCUIT DEVICES AND MODELLING</b>	<b>1</b>
1.1	Semiconductors and pn Junctions	1
1.2	MOS Transistors	16
1.3	Advanced MOS Modelling	39
1.4	Bipolar-Junction Transistors	42
1.5	Device Model Summary	56
1.6	SPICE-Modelling Parameters	61
1.7	Appendix	65
1.8	References	78
1.9	Problems	78
<b>CHAPTER 2</b>	<b>PROCESSING AND LAYOUT</b>	<b>82</b>
2.1	CMOS Processing	82
2.2	Bipolar Processing	95
2.3	CMOS Layout and Design Rules	96
2.4	Analog Layout Considerations	105
2.5	Latch-Up	118
2.6	References	121
2.7	Problems	121
<b>CHAPTER 3</b>	<b>BASIC CURRENT MIRRORS AND SINGLE-STAGE AMPLIFIERS</b>	<b>125</b>
3.1	Simple CMOS Current Mirror	125
3.2	Common-Source Amplifier	128
3.3	Source-Follower or Common-Drain Amplifier	129
3.4	Common-Gate Amplifier	132
3.5	Source-Degenerated Current Mirrors	135
3.6	High-Output-Impedance Current Mirrors	137
3.7	Cascode Gain Stage	140
3.8	MOS Differential Pair and Gain Stage	142
3.9	Bipolar Current Mirrors	146
3.10	Bipolar Gain Stages	149

- 3.11 Frequency Response 154
- 3.12 SPICE Simulation Examples 169
- 3.13 References 176
- 3.14 Problems 176

## **CHAPTER 4 NOISE ANALYSIS AND MODELLING 181**

- 4.1 Time-Domain Analysis 181
- 4.2 Frequency-Domain Analysis 186
- 4.3 Noise Models for Circuit Elements 196
- 4.4 Noise Analysis Examples 204
- 4.5 References 216
- 4.6 Problems 217

## **CHAPTER 5 BASIC OPAMP DESIGN AND COMPENSATION 221**

- 5.1 Two-Stage CMOS Opamp 221
- 5.2 Feedback and Opamp Compensation 232
- 5.3 SPICE Simulation Examples 251
- 5.4 References 252
- 5.5 Problems 253

## **CHAPTER 6 ADVANCED CURRENT MIRRORS AND OPAMPS 256**

- 6.1 Advanced Current Mirrors 256
- 6.2 Folded-Cascode Opamp 266
- 6.3 Current-Mirror Opamp 273
- 6.4 Linear Settling Time Revisited 278
- 6.5 Fully Differential Opamps 280
- 6.6 Common-Mode Feedback Circuits 287
- 6.7 Current-Feedback Opamps 291
- 6.8 SPICE Simulation Examples 295
- 6.9 References 299
- 6.10 Problems 300

## **CHAPTER 7 COMPARATORS 304**

- 7.1 Using an Opamp for a Comparator 304
- 7.2 Charge-Injection Errors 308
- 7.3 Latched Comparators 317
- 7.4 Examples of CMOS and BiCMOS Comparators 321
- 7.5 Examples of Bipolar Comparators 328
- 7.6 References 330
- 7.7 Problems 331



<b>CHAPTER 8</b>	<b>SAMPLE AND HOLDS, VOLTAGE REFERENCES, AND TRANSLINEAR CIRCUITS</b>	<b>334</b>
8.1	Performance of Sample-and-Hold Circuits	334
8.2	MOS Sample-and-Hold Basics	336
8.3	Examples of CMOS S/H Circuits	343
8.4	Bipolar and BiCMOS Sample and Holds	349
8.5	Bandgap Voltage Reference Basics	353
8.6	Circuits for Bandgap References	357
8.7	Translinear Gain Cell	364
8.8	Translinear Multiplier	366
8.9	References	368
8.10	Problems	370
<b>CHAPTER 9</b>	<b>DISCRETE-TIME SIGNALS</b>	<b>373</b>
9.1	Overview of Some Signal Spectra	373
9.2	Laplace Transforms of Discrete-Time Signals	374
9.3	z-Transform	377
9.4	Downsampling and Upsampling	379
9.5	Discrete-Time Filters	382
9.6	Sample-and-Hold Response	389
9.7	References	391
9.8	Problems	391
<b>CHAPTER 10</b>	<b>SWITCHED-CAPACITOR CIRCUITS</b>	<b>394</b>
10.1	Basic Building Blocks	394
10.2	Basic Operation and Analysis	398
10.3	First-Order Filters	409
10.4	Biquad Filters	415
10.5	Charge Injection	423
10.6	Switched-Capacitor Gain Circuits	427
10.7	Correlated Double-Sampling Techniques	433
10.8	Other Switched-Capacitor Circuits	434
10.9	References	441
10.10	Problems	443
<b>CHAPTER 11</b>	<b>DATA CONVERTER FUNDAMENTALS</b>	<b>445</b>
11.1	Ideal D/A Converter	445
11.2	Ideal A/D Converter	447
11.3	Quantization Noise	448
11.4	Signed Codes	452

- 11.5 Performance Limitations 454
- 11.6 References 461
- 11.7 Problems 461

## **CHAPTER 12 NYQUIST-RATE D/A CONVERTERS 463**

- 12.1 Decoder-Based Converters 463
- 12.2 Binary-Scaled Converters 469
- 12.3 Thermometer-Code Converters 475
- 12.4 Hybrid Converters 481
- 12.5 References 484
- 12.6 Problems 484

## **CHAPTER 13 NYQUIST-RATE A/D CONVERTERS 487**

- 13.1 Integrating Converters 487
- 13.2 Successive-Approximation Converters 492
- 13.3 Algorithmic (or Cyclic) A/D Converter 504
- 13.4 Flash (or Parallel) Converters 507
- 13.5 Two-Step A/D Converters 513
- 13.6 Interpolating A/D Converters 516
- 13.7 Folding A/D Converters 519
- 13.8 Pipelined A/D Converters 523
- 13.9 Time-Interleaved A/D Converters 526
- 13.10 References 527
- 13.11 Problems 528

## **CHAPTER 14 OVERSAMPLING CONVERTERS 531**

- 14.1 Oversampling without Noise Shaping 531
- 14.2 Oversampling with Noise Shaping 538
- 14.3 System Architectures 547
- 14.4 Digital Decimation Filters 551
- 14.5 Higher-Order Modulators 555
- 14.6 Bandpass Oversampling Converters 557
- 14.7 Practical Considerations 559
- 14.8 Multi-Bit Oversampling Converters 565
- 14.9 Third-Order A/D Design Example 568
- 14.10 References 571
- 14.11 Problems 572

## **CHAPTER 15 CONTINUOUS-TIME FILTERS 574**

- 15.1 Introduction to  $G_m$ -C Filters 575
- 15.2 Bipolar Transconductors 584

15.3	CMOS Transconductors Using Triode Transistors	597
15.4	CMOS Transconductors Using Active Transistors	607
15.5	BiCMOS Transconductors	616
15.6	MOSFET-C Filters	620
15.7	Tuning Circuitry	626
15.8	Dynamic Range Performance	635
15.9	References	643
15.10	Problems	645

**CHAPTER 16 PHASE-LOCKED LOOPS** **648**

16.1	Basic Loop Architecture	648
16.2	PLLs with Charge-Pump Phase Comparators	663
16.3	Voltage-Controlled Oscillators	670
16.4	Computer Simulation of PLLs	680
16.5	Appendix	689
16.6	References	692
16.7	Problems	693

**INDEX** **696**



sometimes used in digital circuits, where the circle indicates that a low voltage on the gate turns the transistor on, as opposed to a high voltage for an n-channel transistor (Fig. 1.7(a)). The symbols of Fig. 1.8(d) or Fig. 1.8(e) might be used in larger circuits where many transistors are present, to simplify the drawing somewhat. They will not be used in this text.

### Basic Operation

The basic operation of MOS transistors will be described with respect to an n-channel transistor. First, consider the simplified cross sections shown in Fig. 1.9, where the source, drain, and substrate are all connected to ground. In this case, the MOS transistor operates similarly to a capacitor. The gate acts as one plate of the capacitor, and the surface of the silicon, just under the thin insulating  $\text{SiO}_2$ , acts as the other plate.

If the gate voltage is very negative, as shown in Fig. 1.9(a), positive charge will be attracted to the channel region. Since the substrate was originally doped  $p^-$ , this negative gate voltage has the effect of simply increasing the channel doping to  $p^+$ ,

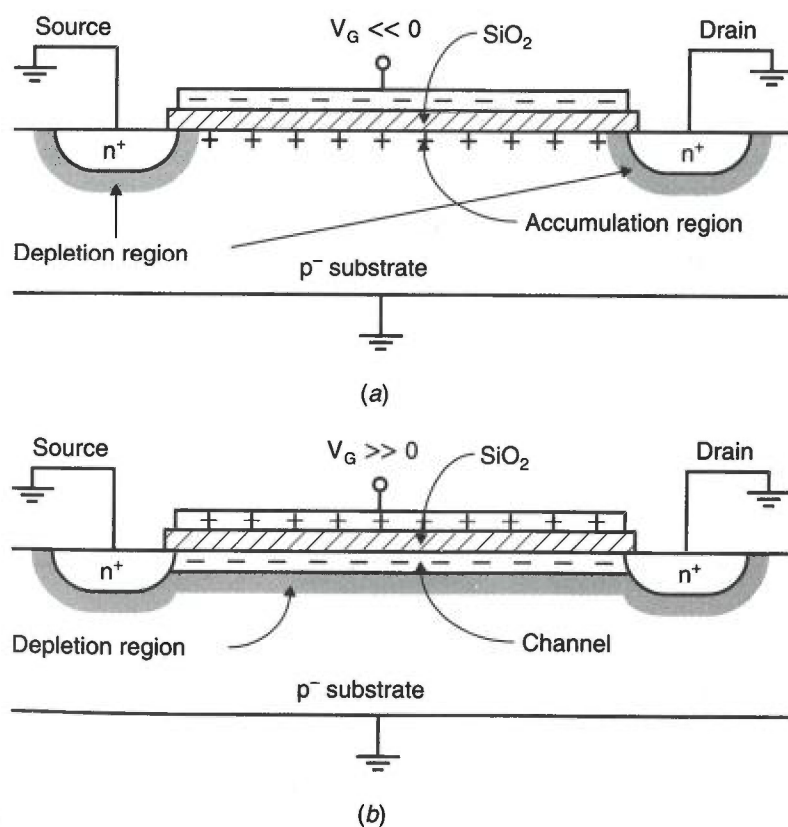


**Fig. 1.9** An n-channel MOS transistor. (a)  $V_G \ll 0$ , resulting in an accumulated channel (no current flow); (b)  $V_G \gg 0$ , and the channel is present (current flow possible from drain to source).

resulting in what is called an *accumulated channel*. The  $n^+$  source and drain regions are separated from the  $p^+$ -channel region by depletion regions, resulting in the equivalent circuit of two back-to-back diodes. Thus, only leakage current will flow even if one of the source or drain voltages becomes large (unless the drain voltage becomes so large as to cause the transistor to break down).

In the case of a positive voltage being applied to the gate, the opposite situation occurs, as shown in Fig. 1.9(b). For small positive gate voltages, the positive carriers in the channel under the gate are initially repulsed and the channel changes from a  $p^-$  doping level to a depletion region. As a more positive gate voltage is applied, the gate attracts negative charge from the source and drain regions, and the channel becomes an  $n$  region with mobile electrons connecting the drain and source regions.<sup>5</sup> In short, a sufficiently large positive gate-source voltage changes the channel beneath the gate to an  $n$  region, and the channel is said to be *inverted*.

The gate-source voltage, for which the concentration of electrons under the gate is equal to the concentration of holes in the  $p^-$  substrate far from the gate, is commonly referred to as the *transistor threshold voltage* and denoted  $V_{tn}$  (for  $n$ -channel transistors). For gate-source voltages larger than  $V_{tn}$ , there is an  $n$ -type channel present, and conduction between the drain and the source can occur. For gate-source voltages less than  $V_{tn}$ , it is normally assumed that the transistor is off and no current flows between the drain and the source. However, it should be noted that this assumption of zero drain-source current for a transistor that is off is only an approximation. In fact, for gate voltages around  $V_{tn}$ , there is no abrupt current change, and for gate-source voltages slightly less than  $V_{tn}$ , small amounts of *subthreshold current* can flow, as discussed in Section 1.3.

When the gate-source voltage,  $V_{GS}$ , is larger than  $V_{tn}$ , the channel is present. As  $V_{GS}$  is increased, the density of electrons in the channel increases. Indeed, the carrier density, and therefore the charge density, is proportional to  $V_{GS} - V_{tn}$ , which is often called the *effective gate-source voltage* and denoted  $V_{eff}$ . Specifically, define

$$V_{eff} \equiv V_{GS} - V_{tn} \quad (1.54)$$

The charge density of electrons is then given by

$$Q_n = C_{ox}(V_{GS} - V_{tn}) = C_{ox}V_{eff} \quad (1.55)$$

Here,  $C_{ox}$  is the gate capacitance per unit area and is given by

$$C_{ox} = \frac{K_{ox}\epsilon_0}{t_{ox}} \quad (1.56)$$

where  $K_{ox}$  is the relative permittivity of  $\text{SiO}_2$  (approximately 3.9) and  $t_{ox}$  is the thickness of the thin oxide under the gate. A point to note here is that (1.55) is only accurate when both the drain and the source voltages are zero.

---

5. The drain and source regions are sometimes called diffusion regions or junctions for historical reasons. This use of the word *junction* is not synonymous with our previous use, in which it designated a pn interface of a diode.

To obtain the total gate capacitance, (1.56) should be multiplied by the effective gate area,  $WL$ , where  $W$  is the gate width and  $L$  is the effective gate length. These dimensions are shown in Fig. 1.10. Thus the total gate capacitance,  $C_{gs}$ , is given by

$$C_{gs} = WLC_{ox} \quad (1.57)$$

and the total charge of the channel,  $Q_{T-n}$ , is given by

$$Q_{T-n} = WLC_{ox}(V_{GS} - V_{tn}) = WLC_{ox}V_{eff} \quad (1.58)$$

The gate capacitance,  $C_{gs}$ , is one of the major load capacitances that circuits must be capable of driving. Gate capacitances are also important when one is calculating *charge injection*, which occurs when a MOS transistor is being turned off because the channel charge,  $Q_{T-n}$ , must flow from under the gate out through the terminals to other places in the circuit.

Next, if the drain voltage is increased above 0 V, a drain-source potential difference exists. This difference results in current flowing from the drain to the source.<sup>6</sup> The relationship between  $V_{DS}$  and the drain-source current,  $I_D$ , is the same as for a resistor, assuming  $V_{DS}$  is small. This relationship is given [Sze, 1981] by

$$I_D = \mu_n Q_n \frac{W}{L} V_{DS} \quad (1.59)$$

where  $\mu_n \cong 0.06 \text{ m}^2/\text{Vs}$  is the mobility of electrons near the silicon surface, and  $Q_n$  is the charge concentration of the channel per unit area (looking from the top down). Note that as the channel length increases, the drain-source current decreases, whereas this current increases as either the charge density or the transistor width increases. Using (1.58) and (1.59) results in

$$I_D = \mu_n C_{ox} \frac{W}{L} (V_{GS} - V_{tn}) V_{DS} = \mu_n C_{ox} \frac{W}{L} V_{eff} V_{DS} \quad (1.60)$$

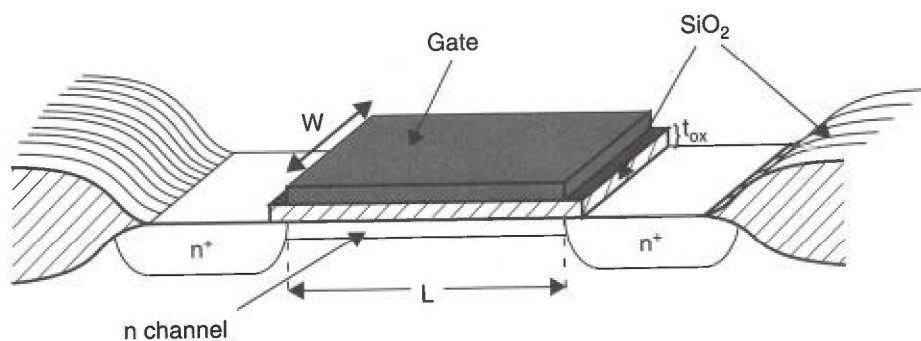


Fig. 1.10 The important dimensions of a MOS transistor.

6. The current is actually conducted by negative carriers (electrons) flowing from the source to the drain. Negative carriers flowing from source to drain results in a positive current from drain to source,  $I_{DS}$ .



where it should be emphasized that this relationship is only valid for drain-source voltages near zero (i.e.,  $V_{DS}$  much smaller than  $V_{eff}$ ).

As the drain-source voltage increases, the channel charge concentration decreases at the drain end. This decrease is due to the smaller gate-to-channel voltage difference across the thin gate oxide as one moves closer to the drain. In other words, since the drain voltage is assumed to be at a higher voltage than the source, there is an increasing voltage gradient from the source to the drain, resulting in a smaller gate-to-channel voltage near the drain. Since the charge density at a distance  $x$  from the source end of the channel is proportional to  $V_G - V_{ch}(x) - V_{tn}$ , as  $V_G - V_{ch}(x)$  decreases, the charge density also decreases.<sup>7</sup> This effect is illustrated in Fig. 1.11.

Note that at the drain end of the channel, we have

$$V_G - V_{ch}(L) = V_{GD} \tag{1.61}$$

For small  $V_{DS}$ , we saw from (1.60) that  $I_D$  was linearly related to  $V_{DS}$ . However, as  $V_{DS}$  increases, and the charge density decreases near the drain, the relationship becomes nonlinear. In fact, the linear relationship for  $I_D$  versus  $V_{DS}$  flattens for larger  $V_{DS}$ , as shown in Fig. 1.12.

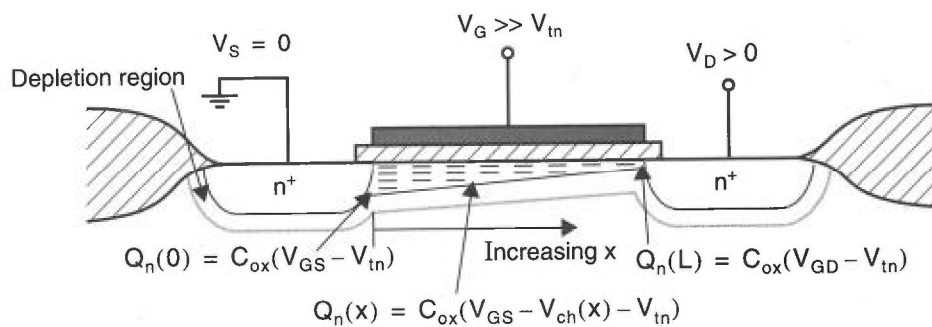


Fig. 1.11 The channel charge density for  $V_{DS} > 0$ .

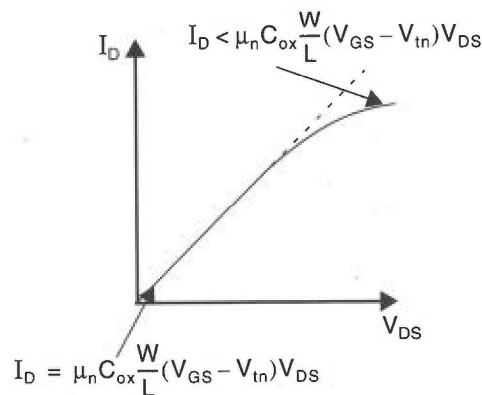


Fig. 1.12 For  $V_{DS}$  not close to zero, the  $I_D$  versus  $V_{DS}$  relationship is no longer linear.

7.  $V_G - V_{ch}(x)$  is the gate-to-channel voltage drop at distance  $x$  from the source end, with  $V_G$  being the same everywhere in the gate, since the gate material is highly conductive.

As the drain voltage is increased, at some point the gate-to-channel voltage at the drain end will decrease to the threshold value  $V_{tn}$ —the minimum gate-to-channel voltage needed for  $n$  carriers in the channel to exist. Thus, at the drain end, the channel becomes *pinched off*, as shown in Fig. 1.13. This pinch-off occurs at  $V_{GD} = V_{tn}$ , since the channel voltage at the drain end is simply equal to  $V_D$ . Thus, pinch-off occurs for

$$V_{DG} > -V_{tn} \quad (1.62)$$

Denoting  $V_{DS-sat}$  as the drain-source voltage when the channel becomes pinched off, we can substitute  $V_{DG} = V_{DS} - V_{GS}$  into (1.62) and find an equivalent pinch-off expression

$$V_{DS} > V_{DS-sat} \quad (1.63)$$

where  $V_{DS-sat}$  is given<sup>8</sup> by

$$V_{DS-sat} = V_{GS} - V_{tn} = V_{eff} \quad (1.64)$$

The electron carriers travelling through the pinched-off drain region are velocity saturated, similar to a gas under pressure travelling through a very small tube. If the drain-gate voltage rises above this critical pinch-off voltage of  $-V_{tn}$ , the charge concentration in the channel remains constant (to a first-order approximation) and the drain current no longer increases with increasing  $V_{DS}$ . The result is the current-voltage relationship shown in Fig. 1.14 for a given gate-source voltage. In the region of operation where  $V_{DS} > V_{DS-sat}$ , the drain current is independent of  $V_{DS}$  and is called the *active region*.<sup>9</sup> The region where  $I_D$  changes with  $V_{DS}$  is called the *triode region*. When MOS transistors are used in analog amplifiers, they almost always are biased in the active region. When they are used in digital logic gates, they often operate in both regions.

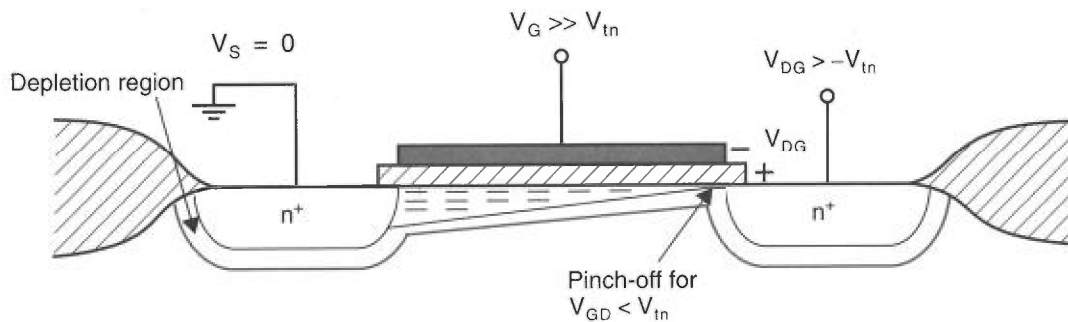


Fig. 1.13 When  $V_{DS}$  is increased so that  $V_{GD} < V_{tn}$ , the channel becomes pinched off at the drain end.

8. Because of the body effect, the threshold voltage at the drain end of the transistor is increased, resulting in the true value of  $V_{DS-sat}$  being slightly lower than  $V_{eff}$ .

9. Historically, the active region was called the saturation region, but this led to confusion because in the case of bipolar transistors, the saturation region occurs for small  $V_{CE}$ , whereas for MOS transistors it occurs for large  $V_{DS}$ . The renaming of the saturation region to the active region is becoming widely accepted.

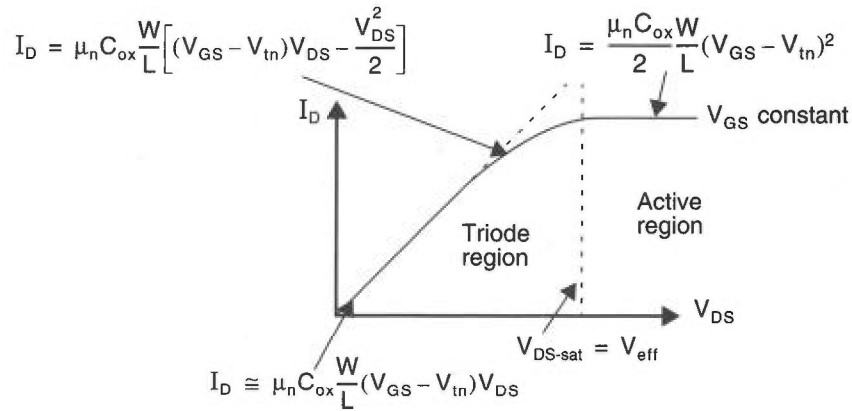


Fig. 1.14 The  $I_D$  versus  $V_{DS}$  curve for an ideal MOS transistor. For  $V_{DS} > V_{DS-sat}$ ,  $I_D$  is approximately constant.

Before proceeding, it is worth discussing the terms *weak*, *moderate*, and *strong inversion*. As just discussed, a gate-source voltage greater than  $V_{tn}$  results in an inverted channel, and drain-source current can flow. However, as the gate-source voltage is increased, the channel does not become inverted (i.e., n-region) suddenly, but rather gradually. Thus, it is useful to define three regions of channel inversion with respect to the gate-source voltage. In most circuit applications, noncutoff MOS-FET transistors are operated in strong inversion, with  $V_{eff} > 100$  mV (many prudent circuit designers use a minimum value of 200 mV). As the name suggests, strong inversion occurs when the channel is strongly inverted. It should be noted that all the equation models in this section assume strong inversion operation. Weak inversion occurs when  $V_{GS}$  is approximately 100 mV or more below  $V_{tn}$  and is discussed as subthreshold operation in Section 1.3. Finally, moderate inversion is the region between weak and strong inversion.

### Large-Signal Modelling

The *triode region equation* for a MOS transistor relates the drain current to the gate-source and drain-source voltages. It can be shown (see Appendix) that this relationship is given by

$$I_D = \mu_n C_{ox} \left( \frac{W}{L} \right) \left[ (V_{GS} - V_{tn}) V_{DS} - \frac{V_{DS}^2}{2} \right] \quad (1.65)$$

As  $V_{DS}$  increases,  $I_D$  increases until the drain end of the channel becomes pinched off, and then  $I_D$  no longer increases. This pinch-off occurs for  $V_{DG} = -V_{tn}$ , or approximately,

$$V_{DS} = V_{GS} - V_{tn} = V_{eff} \quad (1.66)$$

Right at the edge of pinch-off, the drain current resulting from (1.65) and the drain current in the active region (which, to a first-order approximation, is constant with



respect to  $V_{DS}$ ) must have the same value. Therefore, the *active region equation* can be found by substituting (1.66) into (1.65), resulting in

$$I_D = \frac{\mu_n C_{ox}}{2} \left( \frac{W}{L} \right) (V_{GS} - V_{tn})^2 \quad (1.67)$$

For  $V_{DS} > V_{eff}$ , the current stays constant at the value given by (1.67), ignoring second-order effects such as the finite output impedance of the transistor. This equation is perhaps the most important one that describes the large-signal operation of a MOS transistor. It should be noted here that (1.67) represents a squared current-voltage relationship for a MOS transistor in the active region. In the case of a BJT transistor, an exponential current-voltage relationship exists in the active region.

As just mentioned, (1.67) implies that the drain current,  $I_D$ , is independent of the drain-source voltage. This independence is only true to a first-order approximation. The major source of error is due to the channel length shrinking as  $V_{DS}$  increases. To see this effect, consider Fig. 1.15, which shows a cross section of a transistor in the active region. A pinched-off region with very little charge exists between the drain and the channel. The voltage at the end of the channel closest to the drain is fixed at  $V_{GS} - V_{tn} = V_{eff}$ . The voltage difference between the drain and the near end of the channel lies across a short depletion region often called the *pinch-off region*. As  $V_{DS}$  becomes larger than  $V_{eff}$ , this depletion region surrounding the drain junction increases its width in a square-root relationship with respect to  $V_{DS}$ . This increase in the width of the depletion region surrounding the drain junction decreases the effective channel length. In turn, this decrease in effective channel length increases the drain current, resulting in what is commonly referred to as *channel-length modulation*.

To derive an equation to account for channel-length modulation, we first make use of (1.11) and denote the width of the depletion region by  $x_d$ , resulting in

$$\begin{aligned} x_d &\equiv k_{ds} \sqrt{V_{D-ch} + \Phi_0} \\ &= k_{ds} \sqrt{V_{DG} + V_{tn} + \Phi_0} \end{aligned} \quad (1.68)$$

where

$$k_{ds} = \sqrt{\frac{2K_s \epsilon_0}{qN_A}} \quad (1.69)$$

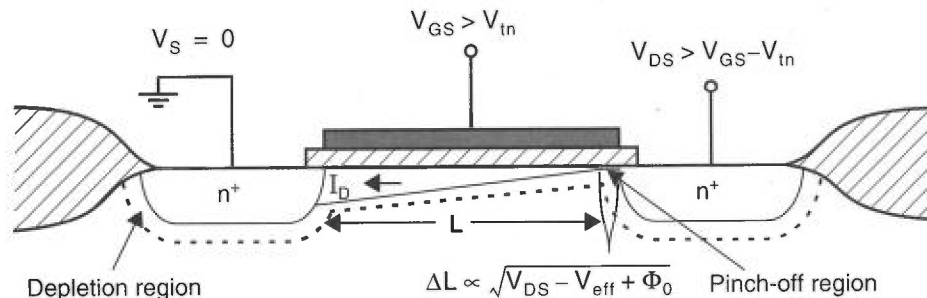


Fig. 1.15 Channel length shortening for  $V_{DS} > V_{eff}$ .

and has units of  $m/\sqrt{V}$ . Note that  $N_A$  is used here since the n-type drain region is more heavily doped than the p-type channel (i.e.,  $N_D \gg N_A$ ). By writing a Taylor approximation for  $I_D$  around its operating value of  $V_{DS} = V_{GS} - V_{tn} = V_{eff}$ , we find  $I_D$  to be given by

$$I_D = I_{D-sat} + \left( \frac{\partial I_D}{\partial L} \right) \left( \frac{\partial L}{\partial V_{DS}} \right) \Delta V_{DS} \cong I_{D-sat} \left( 1 + \frac{k_{ds}(V_{DS} - V_{eff})}{2L\sqrt{V_{DG} + V_{tn} + \Phi_0}} \right) \quad (1.70)$$

where  $I_{D-sat}$  is the drain current when  $V_{DS} = V_{eff}$ , or equivalently, the drain current when the channel-length modulation is ignored. Note that in deriving the final equation of (1.70), we have used the relationship  $\partial L/\partial V_{DS} = -\partial x_d/\partial V_{DS}$ . Usually, (1.70) is written as

$$I_D = \frac{\mu_n C_{ox}}{2} \left( \frac{W}{L} \right) (V_{GS} - V_{tn})^2 [1 + \lambda(V_{DS} - V_{eff})] \quad (1.71)$$

where  $\lambda$  is the output impedance constant (in units of  $V^{-1}$ ) given by

$$\lambda = \frac{k_{ds}}{2L\sqrt{V_{DG} + V_{tn} + \Phi_0}} = \frac{k_{ds}}{2L\sqrt{V_{DS} - V_{eff} + \Phi_0}} \quad (1.72)$$

Equation (1.71) is accurate until  $V_{DS}$  is large enough to cause second-order effects, often called *short-channel effects*. For example, (1.71) assumes that current flow down the channel is not *velocity-saturated* (i.e., increasing the electric field no longer increases the carrier speed). Velocity saturation commonly occurs in new technologies that have very short channel lengths and therefore large electric fields. If  $V_{DS}$  becomes large enough so short-channel effects occur,  $I_D$  increases more than is predicted by (1.71). Of course, for quite large values of  $V_{DS}$ , the transistor will eventually break down.

A plot of  $I_D$  versus  $V_{DS}$  for different values of  $V_{GS}$  is shown in Fig. 1.16. Note that in the active region, the small (but nonzero) slope indicates the small dependence of  $I_D$  on  $V_{DS}$ .

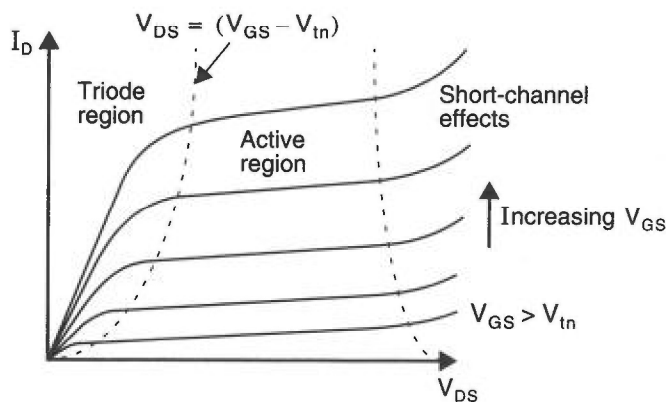


Fig. 1.16  $I_D$  versus  $V_{DS}$  for different values of  $V_{GS}$ .